

Circular magnetic x-ray dichroism in crystalline and amorphous GdFe₂

J. C. Lang,* Xindong Wang, V. P. Antropov, B. N. Harmon, and A. I. Goldman
Ames Laboratory and Department of Physics and Astronomy, Iowa State University, Ames, Iowa 50011

H. Wan and G. C. Hadjipanayis
Department of Physics, University of Delaware, Newark, Delaware 19716

K. D. Finkelstein
Cornell High Energy Synchrotron Source and Department of Applied Engineering Physics,
Cornell University, Ithaca, New York 14853
(Received 22 October 1993)

The spin-dependent absorption of circularly polarized x rays at the *K* edge of Fe and the *L*₂ and *L*₃ edges of Gd in amorphous and crystalline GdFe₂ has been studied. Large differences in the magnitude of the dichroic signal are observed between the two samples. The application of recently derived sum rules indicates substantial quenching of the orbital moment in the amorphous sample. The results are compared to a theoretical spectrum for crystalline GdFe₂.

INTRODUCTION

With the availability of present and next-generation synchrotron radiation sources, circular magnetic x-ray dichroism (CMXD) has increasingly been used as a probe of the bulk magnetic properties of a variety of crystalline¹⁻⁵ and multilayer systems.^{6,7} CMXD is defined as the difference, $\mu_c = \mu^+ - \mu^-$, between the absorption of left and right circularly polarized x-ray beams by a magnetized sample, with μ^+ (μ^-) representing the absorption for x rays with the wave vector parallel (antiparallel) to the ferromagnetically ordered magnetic moment. Since x-ray absorption involves transitions from well-understood core levels with well-defined angular momenta, observed structure in the dichroic spectra can yield information about the ground-state spin polarization and spin-orbit coupling of final states.⁸ Further, the information obtained is element and orbital specific since the technique requires scanning through a specific absorption edge.

To become a useful tool for probing electronic and magnetic structures, CMXD spectra should also be material specific, i.e., sensitive to the changes in the band structure produced by different local environments. Recently, such sensitivity has been demonstrated in a variety of Ho compounds by Fischer *et al.*⁹ In this paper, we compare the CMXD spectra of amorphous GdFe₂ with its crystalline counterpart and a first-principles theoretical calculation of the dichroic spectra for crystalline GdFe₂. First-principles calculations of the dichroic spectra are made possible due to the relatively straightforward cubic structure of GdFe₂. Changes in coordination and nearest-neighbor distances in glassy GdFe₂ should produce sufficient changes in the electronic structure to be detectable by CMXD measurements. Furthermore, amorphous rare-earth-transition-metal materials are of considerable interest because of their many unique magnetic and magneto-optical properties.^{10,11}

For an understanding of these effects, knowledge of the spin polarization and spin-orbit coupling of individual orbitals is necessary. CMXD analysis is, in principle, well suited to providing such information.

The *L* edge CMXD spectra of transition metals,¹³ including 5*d* impurities in 3*d* hosts,¹³ have been well described using a simple spin-polarized band-structure model. Such a model, however, fails to explain the sign, features, and magnitude of the CMXD spectra at the *L*₂ and *L*₃ edges of the rare-earth elements, indicating the need for a more sophisticated interpretation of these spectra. The first measurements of the CMXD spectra performed at the *L* edges of Gd and Tb metal demonstrated two prominent features, one below and one above the absorption edge. The feature above *E_F* (*E_F* is taken as the inflection point in the absorption edge spectra) has been unambiguously assigned to dipolar transitions involving the 5*d* unfilled states of the rare-earth (RE) ion, but the origin of the feature below the edge is still uncertain. Carra and co-workers have suggested that this feature is due to quadrupole transitions to the 4*f* states, pulled below the Fermi energy due to the strong Coulomb interaction between the core hole and these states.¹⁴ As of yet, experiments have not confirmed the quadrupole nature of the feature below *E_F*,^{9,15,16} but recent calculations for all the heavy rare-earth metals by Wang *et al.*¹⁷ that include quadrupole contributions have reproduced the trends seen in the experimental spectra of Ref. 2.

The rare-earth metals are set apart from other magnetic materials by their unique magnetic properties. Their highly localized, partially filled 4*f* shells have negligible overlap with neighboring 4*f* shells and are responsible for large magnetic moments. Magnetic ordering in these materials arises from an exchange coupling between the 4*f* moments and the conduction electrons through which the conduction bands acquire a net magnetization.¹⁸ This exchange is relatively well understood for elemental

rare-earth metals, but intermetallic bonding and spin-orbit coupling complicate the analysis in rare-earth transition metal compounds. A CMXD study can provide key information for understanding the magnetic properties of such materials since CMXD spectra are proportional to the transition matrix elements and the local spin polarization of the final states. In the case of the L_2 and L_3 edges these final states correspond to empty levels within $5d$ bands that are primarily responsible for transmitting the ordering among the $4f$ local moments. In addition, the CMXD spectra at the L_2 and L_3 edges differ from the ratio 1:–1 by an amount dependent upon the spin-orbit coupling in the unoccupied d states.

Quantitative measurements of the degree of coupling are possible by employing recently derived sum rules which relate the integrated intensity of the dichroic, μ_c and normal, μ_0 , absorption coefficients to the ground-state values of the orbital $\langle L_z \rangle$ (Ref. 19) and spin $\langle S_z \rangle$ (Ref. 8) parts of the magnetic moment. Until now, a separate determination of the spin and orbital magnetic moments has been possible only by nonresonant magnetic x-ray scattering.²⁰ Owing to the small size of the magnetic cross section, however, this technique has been limited to samples with large magnetic moments [i.e., Ho $M(4f) = 10\mu_B$, $L = 6$, $S = 2$].²¹ Further, this technique is not orbital specific and requires measurement of several magnetic diffraction peaks with different q values. CMXD, on the other hand, can probe moments on the order of $0.01\mu_B$ with measurements at just the L_2 and L_3 absorption edges. It should also be noted that since the sum rules involve integrated quantities, the values of the moments obtained are ground-state values not affected by the creation of the core hole, which can distort the shape and magnitude of the CMXD spectra.

EXPERIMENTAL DETAILS

The crystalline GdFe_2 sample was prepared by arc-melting 99.99% pure starting materials in a water-cooled copper crucible under argon atmosphere, and was then vacuum annealed for 3 days at 1100°C . The sample was micromilled and standard x-ray diffraction was used to check phase homogeneity. The micromilled sample was distributed uniformly on Kapton tape, with several layers of tape combined to produce a film of approximately 2 absorption thicknesses below the Gd L_3 edge. The amorphous GdFe_2 sample was prepared by sputtering the materials onto a Kapton substrate under vacuum and overlaying the film with a thin ($< 200 \text{ \AA}$) Si layer. The film thickness was found to be $\sim 1.5 \mu\text{m}$ with four films used for the absorption measurements, (~ 1.4 absorption thicknesses just below the Gd L_3 edge). The stoichiometry of the material was checked using energy dispersive spectroscopy and found to be $\text{Gd}_x\text{Fe}_{1-x}$ ($x = 0.315 \pm 0.020$) and standard x-ray-diffraction measurements confirmed the glassy nature of the sample.

The CMXD measurements were taken at the Cornell High-Energy Synchrotron Source bending magnet D line making use of elliptical polarization of the synchrotron beam out of the positron orbital plane. Upstream vertical slits of 0.25 mm (10.2 m from the source) selected radia-

tion which was 0.11 mrad above the positron orbital plane, producing a degree of right circularly polarized light of $P_c \cong 0.66 \pm 0.10$. The beam was diffracted by a double crystal Si (220) monochromator yielding an energy resolution of $\sim 1.5 \text{ eV}$ in the vicinity of the Fe K and Gd L edges where the measurements were performed. In order to eliminate harmonic contamination of the incident beam, the x rays were reflected from a flat quartz mirror placed after the monochromator. The magnetization of the sample was reversed by a 3.5-kG electromagnet, with the magnetic field oriented at 30° with respect to the beam direction.

The polarization of the field was flipped every 2 s at each step in an energy scan through the edges, thus producing two absorption spectra. I^+ is the transmitted intensity when the magnetic moment of the sample and the photon wave vector are in the same direction and I^- is the measured transmitted intensity when the two were in opposite directions. We relate these to the dichroic signal by

$$\mu_c d = \frac{1}{M' P_c \cos\theta} \left[\ln \left[\frac{I_0^+}{I^+} \right] - \ln \left[\frac{I_0^-}{I^-} \right] \right], \quad (1)$$

where I_0^\pm are the incident intensities. In order to account for different experimental conditions and sample characteristics, the data were normalized by the factors found in the denominator of the right-hand side of Eq. (1). Small differences in the thicknesses and stoichiometry were corrected for by normalizing the absorption edge data from the glassy sample to the edge step of the absorption data for the crystalline sample. Further normalization was done by dividing the data by the degree of polarization of the incident beam, P_c and $\cos\theta$, where θ is the angle between the photon beam direction and the magnetic-field direction.

Both crystalline and amorphous GdFe_2 order ferrimagnetically with the iron moment antiparallel to the gadolinium moment. The Curie temperatures are $T_C = 785 \text{ K}$ for the crystalline and $T_C = 500 \text{ K}$ (Ref. 11) for the amorphous sample, yielding reduced temperature values of $T/T_C = 0.38$ and $T/T_C = 0.6$. Therefore, the data must also be corrected for a reduced M' , the fraction of the $T = 0 \text{ K}$ saturation magnetization attained at room temperature for the field employed. Magnetometer measurements performed by us, combined with ferromagnetic resonance measurements by Vittoria, Lubitz, and Ritz²² place the values of the iron and gadolinium sublattice magnetization (room temperature and a 3.5 kG field) at 0.66 ± 0.08 and $0.85 \pm 0.06 M(\text{Fe}, T = 0 \text{ K})_{\text{sat}}$, and 0.67 ± 0.09 and $0.66 \pm 0.08 M(\text{Gd}, T = 0 \text{ K})_{\text{sat}}$ for the crystalline and amorphous samples, respectively. The effective thickness of the sample, d , was determined by matching the experimental edge step with calculated absorption values for crystalline GdFe_2 .²³

RESULTS AND DISCUSSION

The experimental spectra, μ_c , taken in 0.5 eV steps at the Gd L_2 and L_3 edges and the Fe K edge, along with theoretical curves for crystalline GdFe_2 are shown in

Figs. 1–3. A summary of the data is presented in Table I, which displays the integrated intensity and the width of the CMXD signal at each edge, as well as the value of the $5d$ orbital moment determined by using the sum rule derived in Ref. 19.

The relativistic band-structure calculation was carried out within the local spin-density approximation (LSDA) suitable for describing the ground-state properties of heavy rare earths. Dipolar contributions to the dichroism spectra were calculated using an atomic-sphere-approximation tight-binding linear-muffin-tin-orbital (ASA-TB-LMTO) band-structure code with the combined correction,²⁴ and using an atomic model to evaluate quadrupole contributions arising from transitions to the $4f$ states at the Gd L_2 and L_3 edges. The theoretical spectra have been convoluted with a 3.5-eV Lorentzian to account for the finite core hole lifetime. The spectra were also convoluted with a 1.5-eV (full width at half maximum) Gaussian to account for the experimental resolution, and with an energy-dependent broadening to account for the conduction state lifetime.²⁵ The calcula-

tions assume full alignment of the moments. Thus, as stated earlier, we have normalized the experimental data to the $T=0$ K saturation magnetization for direct comparison of theory and experiment.

Only small differences are observed between the amorphous and crystalline spectra at the Fe K edge. Discrepancies between the data sets can be seen 2 eV below the edge (feature *A* in Fig. 1) and 16 eV above the edge (just below feature *D*). The overall magnitude of the dichroism for both samples is approximately the same as indicated by the integrated intensity of features *B* and *C* in Table I. The similarity of the shape and magnitude of the signals suggest that the Fe moment of the amorphous sample is not substantially different from the crystalline sample, although the size of the CMXD signal at the K edge has been shown not to scale with the $3d$ or $4p$ moments in Fe compounds.²⁶ The band-structure calculations attribute features *A*, *B*, and *C* to hybridization between the $4p$ and $3d$ states in the iron. Thus, the difference in feature *A* between the amorphous and crystalline spectra presumably arises from differences in the details of the $4p$ - $3d$ hybridization. The theoretical spec-

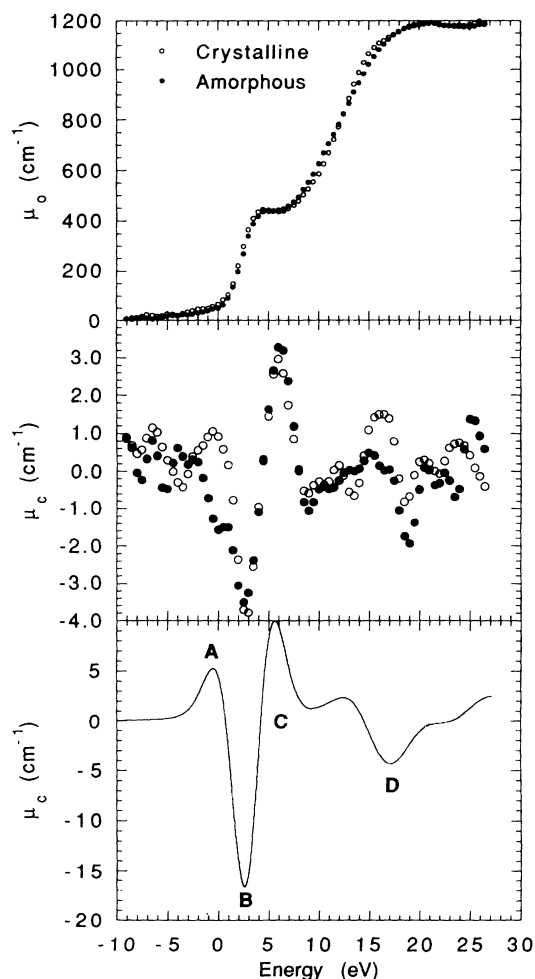


FIG. 1. Dichroism at the Fe K edge. Top: Absorption of crystalline and amorphous samples. Middle: Dichroism signal μ_c of crystalline and amorphous samples. Size of dots indicates approximate error bars. Bottom: Theoretical curve for crystalline GdFe_2 .

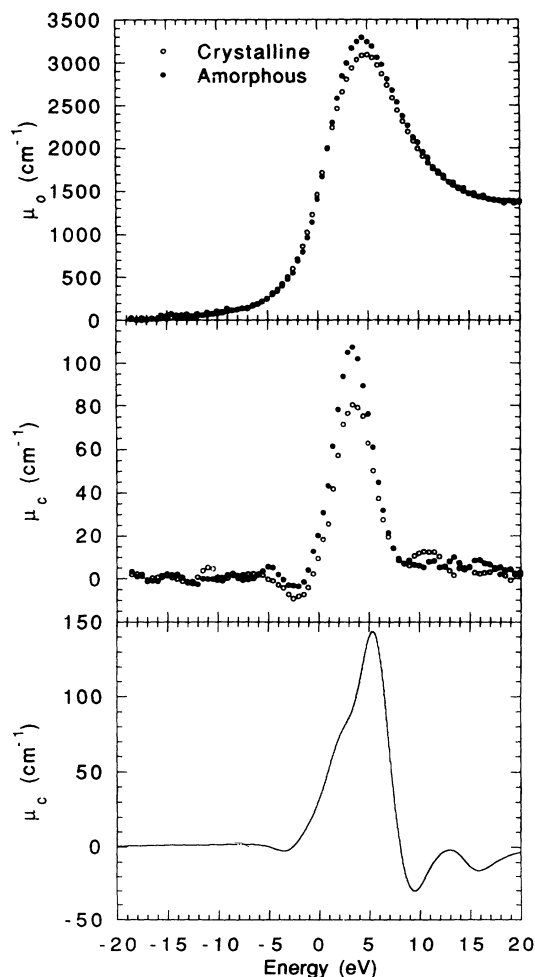


FIG. 2. Dichroism at the Gd L_3 edge. Top: Absorption of crystalline and amorphous samples. Middle: Dichroism signal μ_c of crystalline and amorphous samples. Bottom: Theoretical curve for crystalline GdFe_2 .

TABLE I. Integrated intensities A and widths W for each of the edges. Values for the Fe K edge are for features B and C of Fig. 1. The orbital moments are calculated using the sum rule derived in Ref. 19.

	$A(K)$	$W(K)$ (eV)	$A(L_2)$	$W(L_2)$ (eV)	$A(L_3)$	$W(L_e)$ (eV)	$\langle L_z \rangle$ (μ_B)
Amorphous	-8.0,6.8	2.5,2.0	-465	5.0	508	4.5	0.005±0.003
Crystalline	-7.0,5.7	2.0,2.0	-303	6.0	454	5.0	0.018±0.005
Theory	-34.6,24.8	2.0,2.0	-440	5.5	570	5.0	0.014

trum, while giving a very reasonable match to the shape of experimental crystalline spectrum, overestimates the magnitude of the signal by a factor of 3–4. The theoretical calculations, however, also overestimate the magnitude of the overall absorption by a factor of 1.5, which could account for some of the observed discrepancy.

The sign and magnitude of the dichroism signal at the rare earth L_2 and L_3 edges has been a matter of controversy. Before a discussion of the results of the Gd L edges, then, a brief explanation of the origin of the dichroic signal in these materials is useful. To lowest approximation, the CMXD spectra can be expressed as,

$$\mu_c \propto M(\uparrow)\rho(\uparrow) - M(\downarrow)\rho(\downarrow), \quad (2)$$

where $M(\uparrow(\downarrow))$ is the matrix element for the transition from the $2p$ core level to the spin-up (down) state and $\rho(\uparrow(\downarrow))$ is the density states for majority (minority) spins. In rare-earth compounds the inclusion of distinct matrix elements is essential since the $M(\uparrow)$ matrix elements to the majority spin states are 20–30% larger than the $M(\downarrow)$ matrix elements. This arises from the fact that the $4f$ - $5d$ exchange radially splits the spin bands with the result that the $5d$ spin-up radial functions are larger in magnitude and more contracted at the position of the $2p$ orbitals (see Fig. 8 of Ref. 17). The magnitude of this exchange scales with the spin of the $4f$ states, and is therefore strongest for Gd compounds. A positive net $5d$ moment implies that there are more unoccupied spin-down states above E_F [$\rho(\downarrow) > \rho(\uparrow)$] and therefore one naively expects a net positive (negative) CMXD spectra at the L_2 (L_3) edge. Just the opposite is observed, however, due to the larger $M(\uparrow)$ matrix elements, which make $M(\uparrow)\rho(\uparrow) > M(\downarrow)\rho(\downarrow)$ reversing the sign of the CMXD signal. It should be noted that the expected 1:–1 ratio of the CMXD signal at the L_2 and L_3 edges for systems without conduction electron spin-orbit coupling is not affected since the $2p_{1/2}$ and $2p_{3/2}$ matrix elements differ by less than 10%. Therefore, the difference from the 1:–1 ratio for the CMXD signal at these edges still provides information about the degree of $5d$ conduction electron spin-orbit coupling and the sum rule derived for $\langle L_z \rangle$, as discussed below, still holds.

The difference in the matrix elements is also partly responsible for the observed enhancement of the dichroic signal in the amorphous sample. The Fe coordination around each Gd atom has been determined to be 6.5 ± 0.6 in amorphous GdFe_2 as compared to 12 for the crystalline compound while the nearest-neighbor distances remain roughly the same.²⁷ This smaller coordination number reduces the $5d$ - $3d$ exchange thus diminishing the spin polarization of the $5d$ band. This interpretation is supported by recent calculations performed by Brooks, Nordström, and Johansson²⁸ on a series of $R(\text{Fe})_2$ compounds, where the $3d$ - $5d$ hybridization results in greater $3d$ spin-down (parallel to the RE moment) charge transfer to the rare-earth $5d$ band, and thus a larger $5d$ spin polarization. Smaller degrees of hybridization reduce both the $5d$ and $3d$ moments, but since they are oppositely oriented their sum remains essentially constant. Therefore, while the difference in the spin density of the $5d$ band [$\rho(\uparrow) - \rho(\downarrow)$] is smaller in the amorphous sample, the larger $M(\uparrow)$ matrix elements combined with

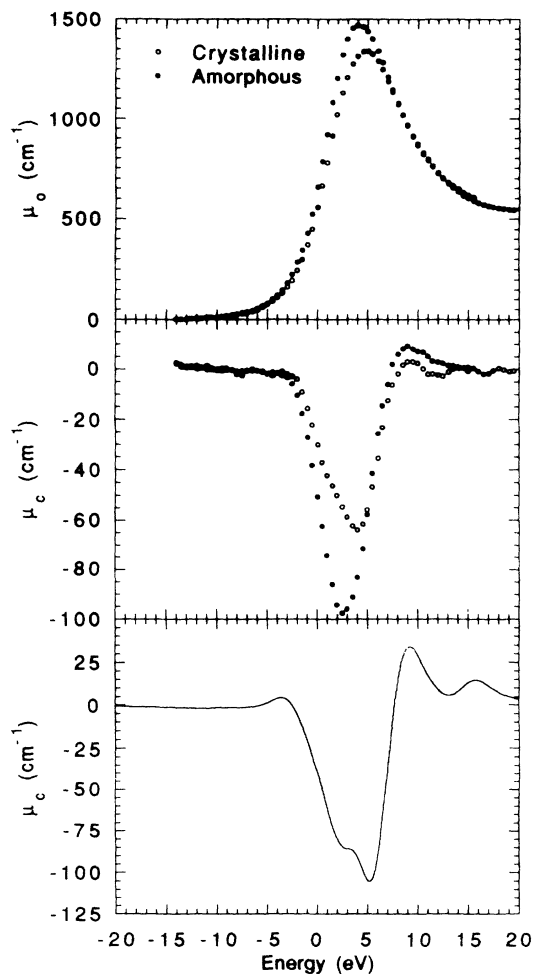


FIG. 3. Dichroism at the Gd L_2 edge. Top: Absorption of crystalline and amorphous samples. Middle: Dichroism signal μ_c of crystalline and amorphous samples. Bottom: Theoretical curve for crystalline GdFe_2 .

the greater number of unoccupied spin-up states above the Fermi energy produces the observed enhanced signal. In this case then, a *smaller* net $5d$ spin moment corresponds to a *larger* CMXD signal.

The sum rules for the CMXD spectra are not affected by the above discussion since they are independent of the matrix elements. At the rare-earth $L_{2,3}$ edges, with initial p ($l=1$) states, final d ($l=2$) states, and $5d$ electron occupancy $N \cong 1.8$ (from the band theory), the sum rules reduce to the following simple expressions:

$$\int_{L_2+L_3} d\omega \mu_c / \int_{L_2+L_3} d\omega 3\mu_0 = 16.4 \langle L_z \rangle \quad (3)$$

and

$$\left\{ \int_{L_3} d\omega \mu_c - 2 \int_{L_2} d\omega \mu_c \right\} / \int_{L_2+L_3} d\omega 3\mu_0 = 12.3 (\langle S_z \rangle + \frac{7}{2} \langle T_z \rangle), \quad (4)$$

with $3\mu_0 \approx \mu^+ + \mu^- + \mu^0$. In the expression above $\langle T_z \rangle$ is the spatial average of the magnetic dipole operator.⁸ While this quantity can be neglected for the transition-metal $3d$ band in $L_{2,3}$ edge CMXD measurements, and calculated analytically for rare-earth $4f$ states in $M_{4,5}$ edge CMXD measurements, it is generally not possible to separate it from $\langle S_z \rangle$ in the expression above for rare-earth $L_{2,3}$ edges. Thus, for the rare-earth $5d$ states a qualitative value of only the orbital moment can be obtained. The value from Eq. (4) above could still be used for orbital specific, field-, and temperature-dependent hysteresis measurements since $\langle S_z \rangle$ and $\langle T_z \rangle$ remain coupled.

The integrated values of the dichroic spectra were obtained by summing the signal over the entire observed energy range at each edge, while the integrated values of μ_0 were determined by modeling the background with a 4-eV broadened arctangent function centered 8.5 eV above the edge. The orbital moment values of 0.018 ± 0.005 and 0.005 ± 0.003 were obtained for the crystalline and amorphous samples, respectively. The uncertainty in the size of the moments arises primarily from the uncertainty in the degree of circular polarization. Since both the amorphous and crystalline data are scaled by this value, the error in relative difference between the amorphous and crystalline samples is $\sim 15\%$ smaller. The smaller value of the $5d$ band spin polarization in the amorphous sample is also responsible, in part, for the substantially smaller $\langle L_z \rangle$ as compared to the crystalline sample, since a smaller net $5d$ moment implies a smaller orbital moment. We believe, however, that the dominant mechanism responsible for the quenching of the orbital moment is the more random crystal-field symmetry present in the amorphous sample. The average crystal field at a particular Gd site should be substantially more asymmetric in the amorphous compound as compared to the crystalline sample leading to decreased effectiveness of the spin-orbit coupling in producing an orbital polarization of the $5d$

conduction bands.

The theoretical dichroic spectra at the L_2 and L_3 edges reproduce the general features observed in the experimental spectra. The theoretical curves, however, show more pronounced structure than experiment. We believe that this is due to the neglect of core-hole effects. The inclusion of core-hole effects would draw in, and narrow, the $5d$ band compressing the signal near the Fermi energy, as observed in experiment. As stated previously, the sum rules are not affected by the core hole, since they involve an integration over all states. The value of the $5d$ orbital moment observed by experiment $0.018 \pm 0.005 \mu_B$ for crystalline GdFe₂ is within error of the value obtained from theory, $0.014 \mu_B$.

In general the calculation of $\langle L_z \rangle$ will be questionable for rare-earth $L_{2,3}$ edges due to the uncertainty in the origin of the feature below the edge. This feature, however, does not carry much spectral weight for Gd and therefore should not significantly affect the observed value. To illustrate this point, we have also applied the sum rules to the theoretical spectra with the proposed quadrupole contributions included in order to more closely approximate the experimental procedure. This yields a value of $0.017 \mu_B$, marginally larger than the theoretical result obtained by excluding the contributions below the edge and well within the experimental error of our measurement. We point out again, however, that the success of these sum rules for determining the orbital moment in most rare-earth magnets will depend strongly on the strength of the feature found below the edge and the identification of its multipolar nature.

We have demonstrated that the differences in the spin-dependent band structure between amorphous and crystalline materials are easily observable by CMXD. Further, it has been shown that the differences can be quantified using the recently derived sum rules to obtain the size of the orbital moments. The degree of spin-orbit coupling present in the sample is consistent with band-structure calculations. This information should prove valuable in analyzing the magnetic and magneto-optical properties of amorphous rare-earth-transition-metal materials. The theoretical calculations are being extended to include estimates of the core-hole effects and the changes in electronic structure for the amorphous ground state. Since these calculations are much more involved, they will be reported elsewhere. We expect that, with the advent of third-generation synchrotron sources, CMXD should become an increasingly important tool to probe the magnetic properties of different magnetic materials.

ACKNOWLEDGMENTS

Ames Laboratory is operated for the United States Department of Energy by Iowa State University under Contract No. W-7405-ENG-82. Work at CHSS was supported by the National Science Foundation under Grant No. DMR-87-19764.

- *Present address: Advanced Photon Source, Bldg. 316, Argonne Natl. Lab., Argonne, IL 60439.
- ¹G. Schütz, M. Knülle, R. Wienke, W. Wilhelm, W. Wagner, P. Kienle, and R. Frahm, *Z. Phys. B* **73**, 67 (1988).
- ²P. Fischer, G. Schütz, and G. Wiesinger, *Solid State Commun.* **76**, 777 (1990).
- ³F. Baudelet, C. Brouder, E. Dartyge, A. Fontaine, J. P. Kappler, and G. Krill, *Europhys. Lett.* **13**, 787 (1990).
- ⁴P. Rudolf, F. Sette, L. H. Tjeng, G. Mięgs, and C. T. Chen, *J. Magn. Magn. Mater.* **109**, 109 (1992).
- ⁵J. Ph. Schille, Ph. Sainctavit, Ch. Cartier, D. Lefebvre, C. Brouder, J. P. Kappler, and G. Krill, *Solid State Commun.* **85**, 787 (1993).
- ⁶S. Rüegg, G. Schütz, P. Fischer, R. Wienke, W. B. Zeper, and H. Ebert, *J. Appl. Phys.* **69**, 5655 (1991).
- ⁷Y. Wu, J. Stöhr, B. D. Hermsmeir, M. G. Samant, and D. Weller, *Phys. Rev. Lett.* **69**, 2307 (1992).
- ⁸P. Carra, B. T. Thole, M. Altarelli, and X. Wang, *Phys. Rev. Lett.* **70**, 694 (1993).
- ⁹P. Fischer, G. Schütz, S. Scherle, M. Knülle, S. Stähler, and G. Wiesinger, *Solid State Commun.* **82**, 857 (1992).
- ¹⁰J. J. Rhyne, in *Handbook on the Physics and Chemistry of Rare Earths*, edited by K. A. Gschneidner, Jr. and L. Eyring (North-Holland, Amsterdam, 1979), Vol. 2, Chap. 16.
- ¹¹K. H. J. Buschow, in *Handbook on the Physics and Chemistry of Rare Earths*, edited by K. A. Gschneidner, Jr. and L. Eyring (North-Holland, Amsterdam, 1983), Vol. 7, Ch. 52.
- ¹²H. Ebert, P. Strange, and B. L. Gyorfly, *J. Appl. Phys.* **63**, 3055 (1988).
- ¹³R. Wienke, G. Schütz, and H. Ebert, *J. Appl. Phys.* **69**, 6147 (1991).
- ¹⁴P. Carra, B. N. Harmon, B. T. Thole, M. Altarelli, and G. A. Sawatzky, *Phys. Rev. Lett.* **66**, 2495 (1991).
- ¹⁵J. C. Lang, S. W. Kycia, X. Wang, B. N. Harmon, A. I. Goldman, D. J. Branagan, R. W. McCallum, and K. D. Finkelstein, *Phys. Rev. B* **46**, 5298 (1992).
- ¹⁶K. Shimomi, H. Maruyama, K. Kobayashi, A. Koizumi, H. Yamazaki, and T. Iwazumi, *Jpn. J. Appl. Phys.* **32-2**, 314 (1992).
- ¹⁷X. Wang, T. C. Lueng, B. N. Harmon, and P. Carra, *Phys. Rev. B* **47**, 9087 (1993).
- ¹⁸See, for example, B. N. Harmon and A. J. Freeman, *Phys. Rev. B* **10**, 1979 (1974), and references therein.
- ¹⁹B. T. Thole, P. Carra, F. Sette, and G. van der Laan, *Phys. Rev. Lett.* **68**, 1943 (1992).
- ²⁰M. Blume and D. Gibbs, *Phys. Rev. B* **37**, 1779 (1988).
- ²¹Doon Gibbs, D.R. Harshman, E. D. Isaacs, D. B. McWhan, D. Mills, and C. Vettier, *Phys. Rev. Lett.* **61**, 1241 (1988).
- ²²C. Vittoria, P. Lubitz, and V. Ritz, *J. Appl. Phys.* **49**, 4908 (1978).
- ²³Values for the absorption were obtained using the ICSC program developed at the University of Washington.
- ²⁴H. L. Skriver, *The LMTO method: muffin-tin orbitals and electronic structure* (Springer-Verlag, New York, 1984).
- ²⁵G. Materlik, J. E. Müller, and J. W. Wilkins, *Phys. Rev. Lett.* **50**, 267 (1983).
- ²⁶S. Stähler, G. Schütz, and H. Ebert, *Phys. Rev. B* **47**, 818 (1993).
- ²⁷G. S. Cargill III, *Solid State Phys.* **30**, 227 (1975).
- ²⁸M. S. S. Brooks, L. Nordström, and B. Johansson, *Physica B* **172**, 95 (1991).